Research in Astronomy and Astrophysics, 22:115018 (7pp), 2022 November https://doi.org/10.1088/1674-4527/ac96b6

Research on the Magnetic Field of NGC 7793 P13 and Other Confirmed Pulsating Ultraluminous X-Ray Sources

Fan-Liang Meng, Yuan-Yue Pan, and Zhao-Sheng Li
Key Laboratory of Stars and Interstellar Medium, Xiangtan University, Xiangtan 411105, China; panyy@xtu.edu.cn
Received 2022 May 10; revised 2022 September 4; accepted 2022 September 20; published 2022 November 2

Abstract

A pulsating ultraluminous X-ray source (PULX) is a new kind of pulsar (PSR) whose characteristics are different from all known neutron stars. The magnetic field of PULX is suspected to be the main reason to support its supper Eddington luminosity of PULX. NGC 7793 P13, which is the second confirmed PULX, can be easily studied due to its nearby position and isolation from other sources in its host galaxy. In this paper, we calculate its magnetic field to be $\sim 1.0 \times 10^{12}$ G based on the continued observations from 2016 to 2020. The magnetic field evolution of NGC 7793 P13 is analyzed, which shows that the source has spent about 10^4 yr for the field decaying from the simulated initial strength 4.0×10^{14} G to the present value. In case of an assumed constant accretion and the limitation of the companion mass, it will be a recycled PSR whose magnetic field is $\sim 10^9$ G and spin period is a few hundred milliseconds. We estimate the field strength of the other confirmed PULXs and find main range is 10^{13}–10^{14} G. Their positions of the magnetic field and spin period are around or below the magnetars. This is because these PULXs are in the binary systems and are with the spin-up rate that are 2–3 orders higher than the normal binary pulsars. We suggest that PULXs are the accreting magnetars whose multi-pole strong magnetic field can support the supper Eddington luminosity. They would be helpful for studying the evolution of the magnetars, the formation of the binary PSRs above the Eddington spin-up line, and the millisecond PSRs with the magnetic field stronger than $\sim 10^9$ G.

Key words: stars: neutron – (stars:) pulsars – stars: evolution – stars: magnetic field – accretion – accretion disks – X-rays: bursts – stars: magnetars

1. Introduction

The pulsating ultraluminous X-ray sources (PULXs) are the accreting pulsars (PSRs) with the luminous in excess of 10^{39} erg s^{-1}. The first confirmed PULX is M82 X-2, which illustrates that there are not only black holes but also neutron stars (NSs) in the ultraluminous X-ray sources (ULXs) (Bachetti et al. 2014; Shao & Li 2015; King & Lasota 2016; King et al. 2017). Up to now more than 10 PULXs have been discovered, which make us believe that there must be more NSs in ULXs (King & Lasota 2020; Song et al. 2020).

The ultra X-ray luminosity and the spin-up rate of the confirmed PULXs are totally different to all known NSs, which are suspected to be attributed to their magnetic field (Bildsten et al. 1997; Frank et al. 2002). Some researches proposed that the magnetic field of the PULXs was in the level of normal PSRs, $\sim 10^{12}$ G (Bachetti et al. 2014; Fürst et al. 2016; Carpano et al. 2018; King & Lasota 2020). The beaming factor could be induced to account for the observed and the real accretion luminosity (Feng & Soria 2011). However, the pulse profiles of the confirmed PULXs were found to be nearly sinusoidal, which denied the existence of the strong beaming (Fürst et al. 2016; Israel et al. 2017b). Thus, other researches suggested that the PULXs were magnetars, whose strong magnetic field in the multi-poles reduced the electron scattering cross section and promoted the luminosity to excess the Eddington limit (Dall'Osso et al. 2015; Eksi et al. 2015; Tong 2015; Pan et al. 2016; Tong & Wang 2019; Chen et al. 2021). Erkut et al. (2020) suggested that both of the magnetic fields ($\sim 10^{12}$ G and $\sim 10^{14}$ G) were possible for PULXs when they considered the spin up rate and luminosity state for each PULX. Kluźniak & Lasota (2015) calculated a weak magnetic field of M82 X-2 to be $\sim 10^9$ G, which illustrated that the accretion disk was closed to the stellar surface. The direct way of determining the field strength of a PSR is by the cyclotron resonant scattering feature (CRSF) in the spectrum. Until now, only one PULX, M51 ULX8, was detected with a certain CRSF, which corresponded to a field strength of $\sim 10^{15}$ G if it was generated by proton (Brightman et al. 2018; Middleton et al. 2019). NGC 300 ULX1 is the other PULX that was detected with a potential CRSF, which indicated a $\sim 10^{12}$ G field strength for the electron CRSF (Carpano et al. 2018; Vasilopoulos et al. 2018; Walton et al. 2018). However, such a CRSF was in doubtful since the spectral and the temporal characteristics of NGC 300 could be described by a model without the absorption feature (Koliopanos et al. 2019).

NGC 7793 P13, located in the Sculptor galaxy at a distance of 3.4 Mpc, is the second PULX confirmed in 2016 (Fürst et al. 2016). Due to its isolation from other sources in the host galaxy and the persistent pulsation, it becomes possible for inspecting the nature and the accretion physics of the source (Read & Pietsch 1998; Zgirski et al. 2017; Fürst et al. 2018; Soria et al. 2020; Walton et al. 2020). With the X-ray observations in 2016 by XMM-Newton and NuSTAR (total exposure time was ∼50 ks and 100 ks, respectively), NGC 7793 P13 was found with a pulse period, P, ∼0.42 s, the spin-up rate, $\dot{P}$, $\sim -3.5\times10^{-11}$ ss^{-1}, and the observed peak luminosity, $L_{\rm X}$, $\sim 10^{40}$ erg s^{-1} (Fürst et al. 2016; Israel et al. 2017b). The dipole magnetic field of NGC 7793 P13 was inferred to be 2×10^{12} G based on the accretion model by Ghosh & Lamb (1979), where the beaming factor $b\sim0.5$ was assumed (Fürst et al. 2016). Tong & Wang (2019) calculated a 2×10^{11} G magnetic field in considering of the accreting low magnetic field magnetar scenario. Erkut et al. (2020) estimated the dipole field strength range was $\sim10^{9}$–10^{12} G with the spin-up rate. Chen et al. (2021) proposed that NGC 7793 P13 was an accreting magnetar. Its magnetic field was preferred to be 10^{12}–10^{14} G when they considered the spin-up process and the equilibrium situation by different torque methods (Chen et al. 2021).

The continued monitoring on NGC 7793 P13 had been carried out by NuSTAR and XMM-Newton in 2018, 2019 and 2020 (Fürst et al. 2021). These observed data can provide more information for studying the magnetic field and the corresponding evolution of the source during the accretion. With the recent observations, we will calculate the magnetic field of NGC 7793 P13 during its spin-up process in Section 2. The field strength of other confirmed PULXs are also estimated in the same section. The evolution of the spin period and the magnetic field is analyzed in Section 3. Discussions and conclusions are given in Sections 4 and 5, respectively.

2. The Magnetic Field Calculation

2.1. The GL Method

In the binary system, the accretion torque $N_{\rm acc}$ of an NS comes from the stresses of the accreting matter at the inner edge of the accretion disk, which is (Ghosh & Lamb 1979, 1992; Ghosh 1995):

$$N_{\rm acc}\simeq \dot{M}\sqrt{GMR_{\rm M}}\,, \tag{1}$$

where G is the gravitational constant, $\dot{M}$ is the accretion rate, M is the mass of NS, and R_M is the magnetosphere radius related to the Alfvén radius $R_{\rm A}$

$$R_{\rm M}=\phi R_{\rm A}, \tag{2}$$

$$R_{\rm A}=3.5\times10^{8}m^{-1/7}R_6^{-2/7}L_{37}^{-2/7}\mu_{30}^{4/7}\ {\rm cm}, \tag{3}$$

where ϕ is a model dependent parameter that is assumed to be 0.5 (Teukolsky & Shapiro 1983; Li & Wang 1999; Frank et al. 2002). $\mu_{30}=1/2B_{12}R_6^3$ is the magnetic dipole moment in units of 10^{30} g cm^3, R_6 is the stellar radius in units of 10^6 cm, B_{12} is the polar magnetic field in units of 10^{12} G, m is NS mass in units of solar mass, and L_{37} is the accretion luminosity $L_{\rm acc}$ ($L_{\rm acc}=G\dot{M}M/R$) in units of 10^{37} erg s^{-1}. $N_{\rm acc}$ is associated to the total torque N by the dimensionless torque, $n(\omega_{\rm s})=N/N_0$, which is

$$n(\omega_{\rm s})=1.4\times\left(\frac{1-\omega_{\rm s}/\omega_{\rm c}}{1-\omega_{\rm s}}\right), \tag{4}$$

where $\omega_{\rm s}$ is the fastness parameter

$$\omega_{\rm s}=1.19P^{-1}\dot{M}_{17}^{-3/7}\mu_{30}^{6/7}m^{-5/7}, \tag{5}$$

where $\omega_{\rm c}$ is the critical fastness parameter for the NS in the equilibrium ($n(\omega_{\rm s})=0$), and it was suggested to be 0.35 by Ghosh & Lamb (1979).

The total torque N can generate the change on the angular velocity Ω, $N=I\dot{\Omega}$. Considering the above equations, the spin-up rate can be written in the form as below (Ghosh & Lamb 1979)

$$-\dot{P}\simeq 5.0\times10^{-5}\mu_{30}^{2/7}m^{-3/7}R_6^{6/7}I_{45}^{-1}(PL_{37}^{3/7})^2n(\omega_s)\ {\rm s\ yr^{-1}}, \tag{6}$$

where I_{45} is the moment of inertia I in units of 10^{45} g cm^2. In this work, we apply the standard values of NS mass for a simple case, for instance, $M=1.4M_{\odot}$ and $R=10$ km.

2.2. NGC 7793 P13

The work of Fürst et al. (2021) analyzed four years observations of NGC 7793 P13 form 2016 to 2020 with the monitoring of NuSTAR, XMM-Newton, and Swift. According to these parameters, 14 observations illustrated the source in the spun-up state are chosen and listed in Table 1. It is found that NGC 7793 P13 was spun up less than six milliseconds with a constant long-term spin-up rate (Fürst et al. 2018; Walton et al. 2020). The pulse profile was smooth and sinusoidal instead of narrow and peaked, which indicated the beaming contribution could be neglected and the X-ray luminosity is the accretion luminosity $L_{\rm x}\sim5\times10^{39}$ erg s^{-1} (Fürst et al. 2016). Substituting the values of $L_{\rm X}$, P, and $\dot{P}$ into Equation (6), the magnetic field strengths of NGC 7793 P13 are calculated. The results of B, $\omega_{\rm s}$ and $R_{\rm A}$ are listed in Table 1. We find that the magnetic field appears a decay tendency from 1.3×10^{12} G to 9.4×10^{11} G, which is less than one order of magnitude in an observed time span of ∼ 4 yr. With the mean values of the spin-up rate, $\dot{P}\sim-3.8\times10^{-11}$ s s^{-1}, the pulse period, $P\sim415$ ms, the dipole magnetic field of NGC 7793 P13 is inferred to be 1.04×10^{12} G with a fastness parameter $\omega_{\rm s}\simeq0.12$. It is almost consistent with the result by Fürst et al. (2016).

Table 1
The Magnetic Field Strength of NGC 7793 P13 Calculated by the Observed Parameters

Number	Mission	Epoch	ObsID	Date (MJD)	P(ms)	$\dot{P}$(10^{-10}s s^{-1})	$B(10^{12}$ G)	ω_s	$R_A(10^7$ cm)
1	XMM-Newton	X3/2014	0 748 390 901	57 002.00	418.3900	$-0.5^{+3.0}_{-2.5}$	1.30	0.14	4.87
2	NuSTAR	XN1/2016	80 201 010 002	57 528.18	416.9515	$-0.04^{+0.19}_{-0.17}$	1.22	0.13	4.69
3	XMM-Newton	2017B	0 804 670 301	57 893.66	415.864	$-1.1^{+1.6}_{-3.2}$	1.13	0.13	4.50
4	NuSTAR	2017B	30 302 005 002	57 892.71	415.8755	$-1.39^{+0.27}_{-0.22}$	1.14	0.13	4.51
5	XMM-Newton	2017C	0 804 670 401	57 904.90	415.724	-2 ± 6	1.13	0.13	4.48
6	XMM-Newton	2017E	0 804 670 601	57 924.11	415.669	-6^{+12}_{-5}	1.12	0.12	4.47
7	XMM-Newton	2017I	0804670701	58 083.00	415.214	$-1.0^{+2.4}_{-2.6}$	1.07	0.12	4.35
8	NuSTAR	2017G	30 302 005 004	58 082.95	415.2153	$-1.23^{+0.31}_{-0.24}$	1.07	0.12	4.35
9	XMM-Newton	2018A	0 823 410 301	58 449.79	413.6220	-0^{+11}_{-10}	0.95	0.11	4.09
10	XMM-Newton	2018B	0 823 410 401	58 479.60	413.5800	-3^{+11}_{-10}	0.95	0.11	4.09
11	XMM-Newton	2019A	0 840 990 101	58 619.99	413.1570	-1 ± 5	0.95	0.11	4.08
12	NuSTAR	2019B	50 401 003 002	58 805.68	412.6350	$-1.8^{+1.0}_{-0.8}$	0.94	0.11	4.08
13	XMM-Newton	2019B	0 853 981 001	58 809.36	412.5860	$-1.5^{+2.4}_{-2.5}$	0.94	0.11	4.08
14	NuSTAR	2020A	30 502 019 004	58 856.54	412.5787	$-0.0^{+0.7}_{-0.5}$	0.94	0.11	4.07

Note. Fourteen observations of NGC 7793 P13 monitored by XMM-Newton and NuSTAR, which are chosen from the work of Fürst et al. (2021). The epoch labels are the archival data that can be found in Fürst et al. (2016) and Walton et al. (2018). With the observed parameters of P and $\dot{P}$, the magnetic field B is deduced according to Equation (6). By the inferred fields, the results of R_a and ω_s are given based on Equations (3) and (5).

Table 2
The Magnetic Field Strengths and Observed Parameters of Other Confirmed PULXs

Source	P(s)	$\dot{P}$(s s^{-1})	L_X(erg s^{-1})	B(G)	R_A(cm)	ω_s
M82 X-2[1]	1.37	-2×10^{-10}	1.8×10^{40}	2.74×10^{13}	1.9×10^{8}	0.34
NGC 5907 ULX-1[2]	1.137	$\sim -5.0 \times 10^{-9}$	8.5×10^{40}	3.06×10^{13}	1.3×10^{8}	0.23
NGC 300 ULX-1[3]	31.6	-5.56×10^{-7}	4.7×10^{39}	3.89×10^{14}	1.3×10^{9}	0.25
NGC 1313 X-2	$\sim$1.5	-1.38×10^{-8}	$\sim 2.0 \times 10^{40}$	6.82×10^{14}	1.2×10^{9}	$\sim$0
Swift J0243.6+6124[5]	9.86	-2.1×10^{-8}	$\sim 2.0 \times 10^{39}$	4.93×10^{13}	5.0×10^{8}	0.20
SMC X-3[6]	7.78	-6.46×10^{-9}	1.2×10^{39}	3.33×10^{13}	4.6×10^{8}	0.23
NGC 2403 ULX[7]	$\sim$17.57	-1×10^{-7}	1.2×10^{39}	7.55×10^{12}	5.3×10^{8}	0.07
RX J0209.6-7427[8]	9.28	-1.75×10^{-8}	1.6×10^{39}	2.00×10^{13}	3.3×10^{8}	0.11
M51 ULX-7[9]	2.8	-1.5×10^{-10}	4×10^{39}	3.02×10^{13}	3.1×10^{8}	0.34
M51 ULX-8[10]	...	...	2×10^{39}	$\sim 10^{15}$	...	...

Note. [1] Bachetti et al. (2014); [2] Israel et al. (2017a), Fürst et al. (2017); [3] Carpano et al. (2018), Vasilopoulos et al. (2018); [4] Sathyaprakash et al. (2019); [5] Kennea et al. (2017), Jenke & Wilson-Hodge (2017), Doroshenko et al. (2018), Kong et al. (2022); [6] Weng et al. (2017), Tsygankov et al. (2017), Townsend et al. (2017); [7] Trudolyubov et al. (2007); [8] Iwakiri et al. (2019), Chandra et al. (2020), Vasilopoulos et al. (2020); [9] Castillo et al. (2020); [10] Brightman et al. (2018).

2.3. Other 10 PULXs

There have been confirmed 11 PULXs from 2014 to 2022. Here we list the observed parameters of the other 10 PULXs except NGC 7793 P13 in Table 2 with the target of calculating their magnetic fields according to the same method above. As having been investigated and studied by many researches, the pulse phases of these PULXs are almost sinusoidal, which make us assume a simple case that all the X-ray luminosity of the PSRs are the accretion luminosity. Their magnetic field B, fastness parameter ω_s and Alfv én radius R_A are deduced and listed in Table 2. It can be seen that the magnetic field of PULXs are within the range of $\sim 10^{12}$–10^{15} G, which is consistent with the conclusion by Chen et al. (2021) and Gao & Li (2021). However, the main range of the magnetic field estimated by GL method in our work is $\sim 10^{13}$–10^{14} G.

(1) M82 X-2

It was the first confirmed PULX in 2014 by Bachetti et al. (2014), which is also known as NuSTAR J095551+6940.8. The magnetic field had been studied in the range of 10^{12}–10^{14} G with consideration of the beaming (Dall'Osso et al. 2015; Eksi et al. 2015; Tong 2015; Pan et al. 2016). With the seven years observation from 2014 to 2021, Bachetti et al. (2021)

suggested that the mass available to M82 X-2 could support its high luminosity without the beaming. This strongly favored the source to be a highly-magnetized NS. We deduce the magnetic field of M82 X-2 is 2.74×10^{13} G corresponding to $\omega_s \sim 0.34$.

(2) NGC 5907 ULX-1

It is the brightest PULX in the edge-on spiral galaxy NGC 5907 at a distance of about 17.1 Mpc. The X-ray luminosity is almost $\sim 10^{41}$ erg s^{-1}, which is accreting more than 500 times the Eddington rate. With a detailed analysis of the broadband spectrum during the bright phase in 2014 (Fürst et al. 2017), we consider the accreting luminosity to be 8.5×10^{40} erg s^{-1}. According to the observation by Israel et al. (2017a), a spin-up rate of -5.0×10^{-9} s s^{-1} is chosen. The referred magnetic field is 3.05×10^{13} G.

(3) NGC 300 ULX-1

Among the confirmed PULXs, NGC 300 ULX-1 is with the slowest spin period and a high sin-up rate that is ever seen (Carpano et al. 2018). It had been detected a possible CRSF in the spectrum at $\sim$13 keV, which indicated a $\sim 10^{12}$ G magnetic field strength in case of the CRSF was produced by electron (Walton et al. 2018). But the CRSF was doubted by Koliopanos et al. (2019), who found a model without the absorption feature that could successfully describe the spectral and temporal characteristics of the source. The magnetic field was analyzed to be $\sim 10^{12}$–10^{14} G (Carpano et al. 2018; Vasilopoulos et al. 2018; Tong & Wang 2019). In this work the observations indicate a strong magnetic field of $>10^{14}$ G, which is consistent with the result of Erkut (2021) and Pan et al. (2022).

(4) NGC 1313 X-2

It is related to a PULX due to the faint pulsations discovered in the long-term XMM-Newton observations by Sathyaprakash et al. (2019). In their work, there were two out of six observations revealing a spin period of $\sim$1.5 s and a pulsed fraction of $\sim$5%. Among the confirmed PULXs, NGC 1313 X-2 is with a fast spin period and a rapid spin-up rate at the same time. With the detected parameters, the calculations of the magnetic field give no solution when ω_s is related to B. These lead to a special consideration of $\omega_s \sim 0$ during the calculation, which reveals a magnetic field of 6.82×10^{14} G.

(5) Swift J0243.6+6124

Swift J0243.6+6124 is the first and the only one PULX confirmed in our Galaxy until now. It is a rapid spin-up NS in a close orbit around a Be early-type star, and was peaking above Eddington luminosity at $\sim 2.0 \times 10^{39}$ erg s^{-1} during the giant outburst from 2017 October to 2018 February (Wilson-Hodge et al. 2018; Beri et al. 2021). The magnetic field was suggested to be $\sim 10^{13}$ G (Doroshenko et al. 2018; Wilson-Hodge et al. 2018). Such a field strength was also proposed by the spin evolution studying using the HXMT data although no evidence was found for a cyclotron feature up to 150 keV (Zhang et al. 2019). In this work, slightly stronger field is calculated, which is 4.93×10^{13} G.

(6) SMC X-3

SMC X-3 is in the Small Magellanic Cloud (SMC), which is the second nearest galaxy and contains abundant high-mass X-ray binaries. It is also known as SXP 7.78 for the discovery of an accreting PSR with a spin period of 7.78 s in 2004 by Edge et al. (2004). Then the source showed a giant type II outburst from 2016 August to 2017 March with an extreme luminosity of 1.2×10^{39} er s^{-1} (Townsend et al. 2017; Tsygankov et al. 2017; Weng et al. 2017). According to the observations, the estimated magnetic field is 10^{13} G.

(7) NGC 2403 ULX

NGC 2403 ULX, also known as CXOU J073709.1+653544, is a PULX with the fastest spin-up rate of $\sim 10^{-7}$ s s^{-1} up to now. It was a transient X-ray PSR discovered and analyzed with the Chandra and XMM-Newton observations in 2004 (Trudolyubov et al. 2007). The luminosity in 0.3–100 keV was estimated to be as high as 1.2×10^{39} erg s^{-1}. The timing analysis revealed a pulsation period from 18.25 s to 17.57 s within two months in 2004. We calculate the field to be 7.55×10^{12} G, which is not very stronger than the normal NS-level magnetic fields $\sim 10^{12}$ G.

(8) RX J0209.6-7427

It is detected with a spin period of $\sim$9.3 s in the Be X-ray system that located in the outer wing of SMC (Iwakiri et al. 2019). By analyzing the data of NuSTAR and NICER, Vasilopoulos et al. (2020) found the source was with a luminosity of $\sim 10^{39}$ erg s^{-1} during the outburst. Using the observations with the Soft X-ray Telescope (SXT) and Large Area X-ray Proportional Counter (LAXPC) instruments on the AstroSat satellite, Chandra et al. (2020) found a rapid spin-up during the outburst and exhibited the ultra luminosity of 1.6×10^{39} erg s^{-1}, which illustrated that RX J0209.6-7427 had features of a PULX. These observed parameters determine the magnetic field to be 2.0×10^{13} G by the GL method in our assumption.

(9) M51 ULX-7

It is a 2.8 s PULX observed at an X-ray luminosity between 10^{39} erg s^{-1} and 10^{40} erg s^{-1}, and located in the spiral galaxy M51 at a distance of 8.6 Mpc (Castillo et al. 2020). The derived spin-up rate was $\dot{P} \simeq -1.5 \times 10^{-10}$ s s^{-1} based on their 2018 May to June observations. With the weakly beamed emission, Castillo et al. (2020) suggested a moderately magnetic field of the accreting NS in the range of 10^{12}–10^{13} G while our result is slightly stronger, which is 3.02×10^{13} G, without the beaming effect.

(10) M51 ULX-8

ULX-8 is one of the brightest ULXs in the galaxy M51, whose X-ray luminosity was $\sim 2 \times 10^{39}$ erg s^{-1} in the assumption of isotropic emission. It was identified to be a PULX with

a strong absorption line at 4.5 keV in the Chandra spectrum, which was a CRSF produced by the strong magnetic field of an NS (Brightman et al. 2018). Since the line was narrower than any electron CRSFs previously observed, they preferred it was scattering off proton, which implied a magnetar-level field strength of $\sim 10^{15}$ G.

3. Analysis of the Field Decay

The evolution of the accretion of PSR has been widely studied. In the X-ray binary system, the accretion-induced the magnetic field decay was first proposed by Taam and van den Heuvel in 1986, who discovered the inverse correlation between the field deduction and the accretion mass (Taam & Van den Heuvel 1986). Based on their work, Shibazaki et al. (1989) analyzed the observational data of γ-ray bursts and millisecond pulsars. They suggested an empirical formula for the magnetic field decay when the PSR was in a mass accretion process. Van den Heuvel & Bitzaraki (1995) proposed a minimum field $\sim 10^8$ G of the binary PSR due to the accumulation of the accretion material where the NS magnetosphere radius matched the stellar radius. Assuming the magnetic field lines frozen in the NS crust, the analytic solution about the field decay by accreting was proposed (Zhang & Kojima 2006, hereafter the ZK model). Focusing on the field decay processed, Igoshev et al. (2021) reviewed the theoretical models of the magnetic field evolution of NSs, and discussed several types of NSs that were in favor of magnetic field evolution from the observations.

With the 4 yr observation of NGC 7793 P13, we can study its field decay and the period spun. In order to analyze the magnetic field evolution, the ZK model is employed. The model assumes there is a steady accretion of the PSR in the binary system. Assuming the conservation of the magnetic flux and the frozen of the magnetic field lines on the entire NS crust, the accretion material flows from the polar cap to the equator, will give the dilution of the field strength in the polar zone and the compression of the magnetosphere. When the magnetosphere radius equals to the stellar radius, the bottom strength $B_{\rm f}$ appears. The decayed magnetic field of the PSR during the accretion can be expressed as (Zhang & Kojima 2006)

$$B = \frac{B_{\rm f}}{\{1 - [C/\exp(y-1)]^2\}^{7/4}}, \quad (7)$$

where the parameter $y = 2\xi\Delta M/7M_{\rm cr}$, $\Delta M = \dot{M}t_{\rm ac}$ is the accretion mass determined by the accretion rate $\dot{M}$ and the accretion time $t_{\rm ac}$, $M_{\rm cr}$ is the crust mass that can be taken as $0.2M_{\odot}$. The efficiency factor ξ expresses the frozen flow of the magnetic line due to the plasma instability, which is assumed to be one unit of order for the completely frozen of the magnetic field lines. $C = 1 + (1 - X_0^2)^{1/2} \sim 2$, where $X_0^2 = (B_{\rm f}/B_0)^{4/7}$, B_0 is the initial magnetic field at the beginning of the evolution, and $B_{\rm f}$ is

$$B_{\rm f} = 1.32 \times 10^8 \times \left(\frac{\dot{M}}{\dot{M}_{\rm Edd}}\right)^{1/2} m^{1/4} R_6^{-5/4} \phi^{-7/4}, \quad (8)$$

where $\dot{M}_{\rm Edd}$ is the Eddington accretion rate, $\phi = 0.5$ denotes the ratio of the magnetosphere radius to the Alfvén radius (Zhang & Kojima 2006).

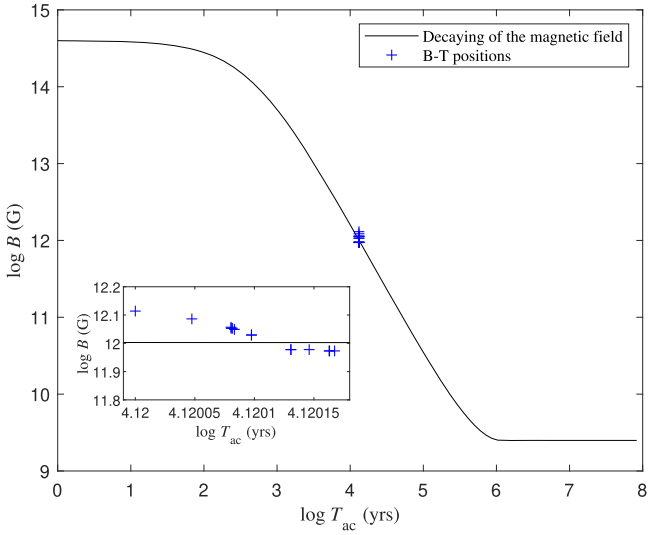

Figure 1. The magnetic field decayed time with the accretion of NGC 7793 P13. The evolution is assumed to begin with $T_{\rm ac} = 0$ and $B_0 = 4.0 \times 10^{14}$ G. The track plotted with the solid line shows the magnetic field decays to the bottom value of $\sim 2.5 \times 10^9$ G with about 10^6 yr. The $B - T_{\rm ac}$ positions are plotted with the referred field value in Table 1 in crossings. The enlarged image of the PSR positions to the evolved track is embedded.

During the analysis of the magnetic field declined with the accretion time for NGC 7793 P13, we consider a constant accretion rate of $\sim 2.7 \times 10^{19}$ g s^{-1} corresponding to the X-ray luminosity of 5.0×10^{39} erg s^{-1}. A caution is that the observed time of $\sim$4 yr is part of the accretion time. Only with the joint effort of the observed time and the calculated magnetic fields, there will be a suitable evolved track of $B - T_{\rm ac}$. The initial field B_0 should not be less than the calculated values. We explore the tracks $B - T_{\rm ac}$ with different B_0 in the sufficient accretion time about 10^8 yr, and the deduced chi-square test is followed tightly with the simulated and the deduced magnetic fields at the same time. Then a track with $B_0 \sim 4 \times 10^{14}$ G is found to be an appropriate trace for NGC 7793 P13, around which are the $B - T_{\rm ac}$ positions with the corresponding values listed in Table 1. In this case, the reduced chi-square is $\sim$1. The $B - T_{\rm ac}$ evolution is plotted in Figure 1, where the embedded image is the enlarged picture of the source positions compared to the evolved track. We see that the source has spent about 10^4 yr evolving from $B_0 \sim 4.0 \times 10^{14}$ G to the present field strength $\sim 1.0 \times 10^{12}$ G, and will decay to the bottom magnetic field of 2.5×10^9 G in about 10^6 yr.

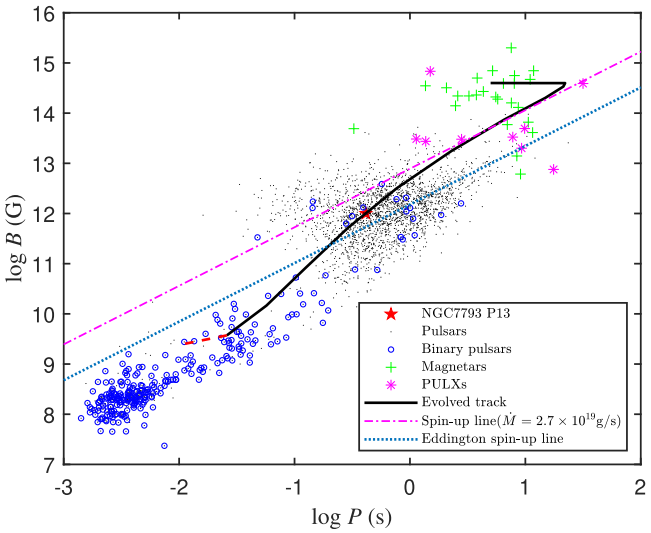

Figure 2. The B-P evolution of NGC 7793 P13. The track with the constant accretion rate $\dot{M} = 2.7 \times 10^{19}$ g s^{-1} is plotted with the curved line. The dashed line is the evolved results limited be $T_{\rm ac}^{\rm limit}$. The star is the B-P position of NGC 7793 P13 with $B = 10^{12}$ G, $P = 415$ ms. The "*" symbols are the other confirmed PULXs. The dots, circles, and crossings represent pulsars, binary pulsars, and magnetars, respectively. The dashed–dotted line and dotted line are the spin-up lines with the accretion rate of 2.7×10^{19} g s^{-1} and 1.0×10^{18} g s^{-1}, respectively.

In general, the accretion time $t_{\rm ac}$ of a binary PSR (BPSR) is related to the lifetime $T_{\rm MS}$ of the companion star in the main sequence (Teukolsky & Shapiro 1983)

$$t_{\rm ac} = \zeta T_{\rm MS}, \tag{9}$$

where the parameter $\zeta \sim 0.1$. The relationship between $T_{\rm MS}$ and the companion mass $M_{\rm c}$ is

$$T_{\rm MS} = 1.3 \times 10^{10}({\rm yr})\left(\frac{M_{\rm c}}{M_{\odot}}\right)^{-2.5}. \tag{10}$$

It had been found NGC 7793 P13 is with a 18–23$M_{\odot}$ companion (Motch et al. 2014), which indicates a limitation of the accretion time about $t_{\rm ac}^{\rm limit} \simeq (0.5\text{–}1) \times 10^6$ yr according to Equations (9) and (10). Within the limitation, the magnetic field of NGC 7793 P13 will decay to $(3.7\text{–}5.0) \times 10^9$ G under the constant accretion rate of 2.7×10^{19} g s^{-1}.

According to Equations (6) and (7), the evolution of the magnetic field and the spin period of NGC 7793 P13 is simulated. During the simulation, conditions of the magnetic field and spin period in the initial and present status are considered. The evolved B-P path in the curved line is plotted in Figure 2, where the dashed part (in the end of the track) is restricted by the accreting time $t_{\rm ac}^{\rm limit} = (0.5 - 1) \times 10^6$ yr. Within the accretion time, NGC 7793 P13 evolves to a recycled PSR whose spin period is a few hundred milliseconds.

4. Discussions

By employing the GL method, we estimate the magnetic field of NGC 7793 P13 with the 4 yr observations. The field strength of the other 10 confirmed PULXs are also presented using the same method. Although there is a limitation of the PULXs number, the field results still show a mainly range of 10^{13}–10^{14} G. NGC 7793 P13 is now with the weakest field strength but the fastest spin period among all the PULXs.

In the B–P diagram of Figure 2, all the confirmed PULXs, radio PSRs, binary PSRs (BPSRs), and magnetars are plotted, whose data are from deduced field results in the work, the ATNF pulsar catalog and McGill Online Magnetar Catalog (Manchester et al. 2005; Olausen & Kaspi 2014). It is found that the PULXs are distributed around or below the magnetars. The outset track of NGC 7793 P13 is in the zone of magnetars. Its evolution crosses the range of the BPSRs that is above the Eddington spin-up line and ends around the positions of recycled PSRs with the spin period of a few hundred milliseconds.

As we known that there has been found about 30 magnetars, all of that are the isolated stars with the magnetic field about 10^{14}–10^{15} G (Olausen & Kaspi 2014; Kaspi & Beloborodov 2017; Esposito et al. 2021). A few magnetars with slightly weak field strength of about 10^{12} G were suspected undergoing an accretion that induced their field decay (Rea et al. 2010; Zhou et al. 2014; Mereghetti et al. 2015). Yoneda et al. (2020) claimed an accreting magnetar existing in the γ-ray binary system LS 5039, but it was denied by Volkov et al. (2021) for the non-detection of the statistical significant bursts or the quasi-periodic variability from the same data set. The confirmed PULXs are with the similar spin period and luminosity to the magnetars. They are also the accreting PSRs with the giant companions in the binary systems, and are with the rapid spin-up rates that are about 2–3 orders higher than that of the normal BPSRs. From the B–P evolution and the relative location of the PULXs to the magnetars and BPSRs, we propose that the PULXs are the accreting magnetar. The multi-pole strong magnetic fields would be the reason for its ultra-luminosity.

They will be the key sources for studying the magnetar evolution, including the formation of the magnetars with $B \sim 10^{12}$ G. It will also help us to improve the understanding of the evolution of the PSR in high-mass X-ray binary, and explain why source PSRs are above the Eddington spin-up line in the B–P diagram.

5. Conclusions

In this paper, we calculate the present magnetic field of NGC 7793 P13 to be $\sim 10^{12}$ G based on the accretion torque model by Ghosh & Lamb (1979). With the 4 yr observations by NuSTAR and XMM-Newton of NGC 7793 P13, we found its magnetic field decayed less than an order of magnitude in the

observed time. The field decayed with the accretion time shows that the source has experienced $\sim 10^4$ yr for the magnetic field evolved from the initial value $B_0 = 4.0 \times 10^{14}$ G to the present field strength. The evolution of the magnetic field and spin period of NGC 7793 P13 is simulated and the corresponding $B-P$ track is plotted in the $B-P$ diagram. Limited by the companion mass, it will be a recycled PSR with the magnetic field about 4×10^9 G and the spin period about a few hundred milliseconds.

We also deduce the magnetic field of other confirmed PULXs, that are found to be in the range of 10^{13}–10^{14} G. When comparing the evolution of $B-P$ track of NGC 7793 P13 the $B-P$ positions of PULXs to the magnetars and BPSRs, we suggest that PULXs are the accreting magnetar (Bachetti et al. 2014; Pan et al. 2016; Israel et al. 2017c; Tong & Wang 2019). The multi-pole magnetic fields of the source can reduce the electron scattering cross-section and increase the luminosity above the Eddington limit. Since no magnetar has been found in the binary system, these PULXs will be helpful for studying the magnetar evolution including the ones that were suspected to undergo the accretion. For hunting the ULXs and PULXs had been carried on (Song et al. 2020), which will provide us more data and analysis for studying the relation of the PULXs, BPSPs and magnetars.

Acknowledgments

This work was supported by the National Natural Science Foundation of China (12130342, 12273030 and U1938107).

References

Bachetti, M., Harrison, F., Walton, D. J., et al. 2014, Nature, 514, 202
Bachetti, M., Heida, M., Maccarone, T., et al. 2021, arXiv:2112.00339
Beri, A., Naik, S., Singh, K. P., et al. 2021, MNRAS, 500, 565
Bildsten, L., Chakrabarty, D., Chiu, J., et al. 1997, ApJS, 113, 367
Brightman, M., Harrison, F. A., Fürst, F., et al. 2018, NatAs, 2, 312
Carpano, S., Haberl, F., Maitra, C., & Vasilopoulos, G. 2018, MNRAS: Letters, 476, L45
Castillo, G. R., Israel, G. L., Belfiore, A., et al. 2020, ApJ, 895, 60
Chandra, A. D., Roy, J., Agrawal, P., & Choudhury, M. 2020, MNRAS, 495, 2664
Chen, X., Wang, W., & Tong, H. 2021, JHEAp, 31, 1
Dall'Osso, S., Perna, R., & Stella, L. 2015, MNRAS, 449, 2144
Doroshenko, V., Tsygankov, S., & Santangelo, A. 2018, A&A, 613, A19
Edge, W., Coe, M., Corbet, R., Markwardt, C., & Laycock, S. 2004, ATel, 225, 1
Ekşi, K., Andaç, İ., Çıkıntoğlu, S., et al. 2015, MNRAS: Letters, 448, L40
Erkut, M., Türkoğlu, M., Ekşi, K., & Alpar, M. A. 2020, ApJ, 899, 97
Erkut, M. H. 2021, EJST, 27, 7
Esposito, P., Rea, N., & Israel, G. L. 2021, in Timing Neutron Stars: Pulsations, Oscillations and Explosions, ed. T. M. Belloni, M. Méndez, & C. Zhang, Vol. 461 (Berlin: Springer), 97
Feng, H., & Soria, R. 2011, NewAR, 55, 166
Frank, J., King, A., & Raine, D. 2002, Accretion Power in Astrophysics (Cambridge: Cambridge Univ. Press)
Fürst, F., Walton, D., Harrison, F., et al. 2016, ApJL, 831, L14
Fürst, F., Walton, D., Heida, M., et al. 2018, A&A, 616, A186
Fürst, F., Walton, D., Heida, M., et al. 2021, A&A, 651, A75
Fürst, F., Walton, D., Stern, D., et al. 2017, ApJ, 834, 77
Gao, S.-J., & Li, X.-D. 2021, RAA, 21, 196
Ghosh, P. 1995, JApA, 16, 289
Ghosh, P., & Lamb, F. 1979, ApJ, 234, 296
Ghosh, P., & Lamb, F. K. 1992, X-Ray Binaries and Recycled Pulsars (Berlin: Springer), 487
Igoshev, A. P., Popov, S. B., & Hollerbach, R. 2021, Universe, 7, 351
Israel, G., Belfiore, A., Rodriguez, G., et al. 2017c, in Proc. Conf. The X-ray Universe, 2017, 104
Israel, G. L., Belfiore, A., Stella, L., et al. 2017a, Science, 355, 817
Israel, G. L., Papitto, A., Esposito, P., et al. 2017b, MNRAS: Letters, 466, L48
Iwakiri, W., Wolff, M., Vasilopoulos, G., et al. 2019, ATel, 13309, 1
Jenke, P., & Wilson-Hodge, C. 2017, ATel, 10812, 1
Kaspi, V. M., & Beloborodov, A. M. 2017, ARA&A, 55, 261
Kennea, J., Lien, A., Krimm, H., Cenko, S., & Siegel, M. 2017, ATel, 10809, 1
King, A., & Lasota, J.-P. 2016, MNRAS: Letters, 458, L10
King, A., & Lasota, J.-P. 2020, MNRAS, 494, 3611
King, A., Lasota, J.-P., & Kluźniak, W. 2017, MNRAS: Letters, 468, L59
Kluźniak, W., & Lasota, J.-P. 2015, MNRAS: Letters, 448, L43
Koliopanos, F., Vasilopoulos, G., Buchner, J., Maitra, C., & Haberl, F. 2019, A&A, 621, A118
Kong, L.-D., Zhang, S., Zhang, S.-N., et al. 2022, arXiv:2206.04283
Li, X.-D., & Wang, Z.-R. 1999, ApJ, 513, 845
Manchester, R. N., Hobbs, G. B., Teoh, A., & Hobbs, M. 2005, AJ, 129, 1993
Mereghetti, S., Pons, J. A., & Melatos, A. 2015, SSRv, 191, 315
Middleton, M., Brightman, M., Pintore, F., et al. 2019, MNRAS, 486, 2
Motch, C., Pakull, M., Soria, R., Grisé, F., & Pietrzyński, G. 2014, Nature, 514, 198
Olausen, S., & Kaspi, V. 2014, ApJS, 212, 6
Pan, Y., Li, Z., Zhang, C., & Zhong, J. 2022, MNRAS, 513, 6219
Pan, Y., Song, L., Zhang, C., & Tong, H. 2016, MNRAS, 461, 2
Rea, N., Esposito, P., Turolla, R., et al. 2010, Science, 330, 944
Read, A., & Pietsch, W. 1998, arXiv:9810013
Sathyaprakash, R., Roberts, T., Walton, D., et al. 2019, MNRAS: Letters, 488, L35
Shao, Y., & Li, X.-D. 2015, ApJ, 802, 131
Shibazaki, N., Murakami, T., Shaham, J., & Nomoto, K. 1989, Nature, 342, 656
Song, X., Walton, D., Lansbury, G., et al. 2020, MNRAS, 491, 1260
Soria, R., Motch, C., & Pakull, M. W. 2020, ATel, 13751, 1
Taam, R. E., & Van den Heuvel, E. 1986, ApJ, 305, 235
Teukolsky, S. A., & Shapiro, S. L. 1983, Black Holes, White Dwarfs, and Neutron Stars: the Physics of Compact Objects (New York: Wiley)
Tong, H. 2015, RAA, 15, 517
Tong, H., & Wang, W. 2019, MNRAS, 482, 4956
Townsend, L., Kennea, J., Coe, M., et al. 2017, MNRAS, 471, 3878
Trudolyubov, S. P., Priedhorsky, W., & Cordova, F. 2007, AAS Meeting, 210, 41
Tsygankov, S., Doroshenko, V., Lutovinov, A., Mushtukov, A., & Poutanen, J. 2017, A&A, 605, A39
Van den Heuvel, E., & Bitzaraki, O. 1995, A&A, 297, L41
Vasilopoulos, G., Haberl, F., Carpano, S., & Maitra, C. 2018, A&A, 620, L12
Vasilopoulos, G., Ray, P., Gendreau, K., et al. 2020, MNRAS, 494, 5350
Volkov, I., Kargaltsev, O., Younes, G., Hare, J., & Pavlov, G. 2021, ApJ, 915, 61
Walton, D., Bachetti, M., Fürst, F., et al. 2018, ApJL, 857, L3
Walton, D., Furst, F., Heida, M., et al. 2020, ATel, 13791, 1
Weng, S.-S., Ge, M.-Y., Zhao, H.-H., et al. 2017, ApJ, 843, 69
Wilson-Hodge, C. A., Malacaria, C., Jenke, P. A., et al. 2018, ApJ, 863, 9
Yoneda, H., Makishima, K., Enoto, T., et al. 2020, PhRvL, 125, 111103
Zgirski, B., Gieren, W., Pietrzyński, G., et al. 2017, ApJ, 847, 88
Zhang, C. M., & Kojima, Y. 2006, MNRAS, 366, 137
Zhang, Y., Ge, M., Song, L., et al. 2019, ApJ, 879, 61
Zhou, P., Chen, Y., Li, X.-D., et al. 2014, ApJL, 781, L16